Analysis of AVC Measurements

Martin Rottinger
Institute for Microelectronics
TU Vienna
A-1040 Vienna, Austria
rottinger@iue.tuwien.ac.at

Norbert Seifert
Digital Semiconductor
75 Reed Road
Hudson, MA 01749, USA
seifert@uogsrv.hlo.dec.com

Siegfried Selberherr
Institute for Microelectronics
TU Vienna
A-1040 Vienna, Austria
selberherr@iue.tuwien.ac.at

Abstract

The Auger Voltage Contrast (AVC) method is a new electronic probing technique for rapid delineation of pn-junctions. Procedures for automatic extraction of the junction position and the doping distribution from measurement data can be considerably improved with simulations of AVC measurements. This paper describes the analysis of AVC measurements.

1. Introduction

Down scaling the feature size of state-of-the-art semiconductor devices increases the demands on accurate positioning of the doping and creates a need for new methods to measure the doping distribution. One of the recently developed electronic properties probing methods is the Auger Voltage Contrast (AVC) method [1].

In the AVC method a beam of high energetic electrons is focused on the surface of the test device. The kinetic energy of emitted secondary electrons is measured. The measured energy is a function of the surface potential which is caused by the doping in the device.

Simulation of such measurements is a valuable tool for the development and improvement of procedures for automatic extraction of doping distributions from the measurement data and to gain better understanding of the involved physical effects.

2. The AVC method

A beam of high energetic electrons is focused on the surface of a cross-sectioned test device. The device is connected by a contact to ground voltage. The incident electrons generate electron-hole pairs in the semiconductor and a fraction of the secondary electrons has enough kinetic energy to leave the semiconductor.

The built-in potential causes a band bending which is a function of the doping. When the kinetic energy of the emitted secondary electrons is measured and compared to the energy of electrons emitted from an undoped semiconductor a shift can be observed which corresponds to the band bending caused by the doping.

A dipole layer at the surface of the semiconductor caused by surface states and the connected potential also influence the shift in the energy of the emitted secondary electrons. But theoretical studies [1] indicate that this effect is only important for small beam currents. Very small beam currents have to be avoided in actual measurements because the number of emitted secondary electrons which can be used for averaging is too small to produce reliable results.

In the AVC method the locations x_i where the electron beam impinges on the semiconductor surface and x_e where the potential is extracted are varied during a scan, therefore it is not sufficient to look for the location where the second derivative of the potential vanishes to determine the pn-junction position. The second derivative of the extracted potential is a function of the charge caused by the doping ρ^dop and the charge from the injected electrons and the generated electron-hole pairs ρ^inj.

$$\nabla^2\varphi = f\left(\rho^\mathrm{dop}(\,x_\mathrm{e}),\ \rho^\mathrm{inj}(x_\mathrm{i},\ x_\mathrm{e})\right)$$

The zero of the second derivative of the potential is located at the metallurgical junction only if ρ^inj can be neglected. For higher beam currents the zero location shifts considerably from the junction.

3. Extension of MINIMOS-NT

In order to gain better understanding of the physics involved in AVC measurements and to facilitate the interpretation of the results of AVC measurements the device simulator MINIMOS-NT [2] has been enhanced to be capable of simulating such measurements.

Appropriate models were added to the simulator to account for the injection of electrons by the electron beam and the electron-hole pair generation caused by the incident high energy electrons. For modeling the distribution of the injected primary electrons and the generated secondary carriers in lateral and vertical direction Gauß distributions were assumed [3]. The distance of the maximum of the distribution from the surface and the lateral and vertical standard deviations are functions of the energy of the incident electrons. Estimates for the distance of the maximum from the surface and the vertical and lateral standard deviations were taken from Monte Carlo simulations performed by the program SESAME [4].

Variations of the distance of the maximum of the distributions from the device surface and of the standard deviations caused by different electron energies have only very small influence on the surface potential because they are small compared to the diffusion length of the carriers. The most important parameters are the beam current and the average number of electron-hole pairs generated per incident electron.

The simulation of an AVC scan requires a number of runs with varying location of the incident electrons. From the results of the single simulation runs the potential at the location of the electron beam is extracted.

4. Examples

The analyzed devices consist of a block of silicon with side contacts to ground level (see Fig. 1). A constant background doping of 10^{16} cm^{-3} and a varying doping with a maximum value of 10^{19} cm^{-3} were used. The metallurgical junction was located at $x = 0.4$ μm. Fig. 2 shows the doping distribution of the first device. For the second example the n- and p-doping were exchanged.

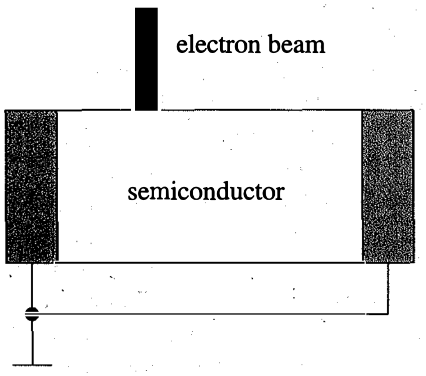

Figure 1. Geometry of the devices.

A constant electron energy of 3 keV was assumed for all calculations and the beam current was varied between 10 pA and 1 nA.

4.1. The p^+n diode

The resulting surface potential is plotted in Fig. 3. On the lower doped side of the pn-junction the vast number of secondary carriers causes a shift in the potential compared to the built-in potential. This decreases the total potential drop across the pn-junction. For all simulated beam currents the surface potential is steepest in the area of the junction. Fig. 4 shows the second derivative of the surface potential.

4.2. The n^+p diode

The surface potential on the lower doped side shows a much stronger change compared to the previous example as can be seen in Fig. 5. For beam currents up to 500 pA the potential drop across the pn-junction is quite large and the slope is steepest near the junction. For 1 nA beam current the potential drop decreases to approximately one fifth of the value for the built-in potential and the slope is very flat and nearly constant in the vicinity of the junction.

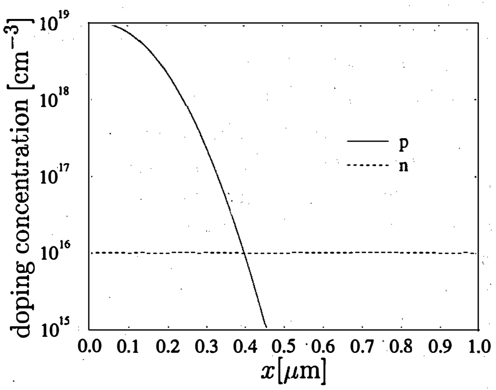

Figure 2. Doping distribution of the p^+n diode. The metallurgical junction is located at $x = 0.4$ μm.

The different changes in the potential for the same beam current for the p^+n and the n^+p diode are caused by the different mobility of electrons and holes. When the electron beam is located on the lower doped side of the pn-junction outside of the space charge region the minority carrier concentration is much higher than in equilibrium. The carriers diffuse away from the location of the beam towards the contacts because of the strong concentration gradient. When the minority carriers reach the space charge region they are pulled across the junction by the built-in electric field, and the potential difference is reduced. In silicon the mobility of electrons is approximately three times larger than the mobility of holes. Therefore the electron current across the junction for the n^+p device is much higher than the hole current for the p^+n diode. Hence, the influence on the potential is much stronger for the n^+p device.

5. Conclusion

From the simulations it is evident that some a-priori knowledge about the doping is necessary to choose a suitable electron beam current and energy of the primary electrons for the measurement. For high electron

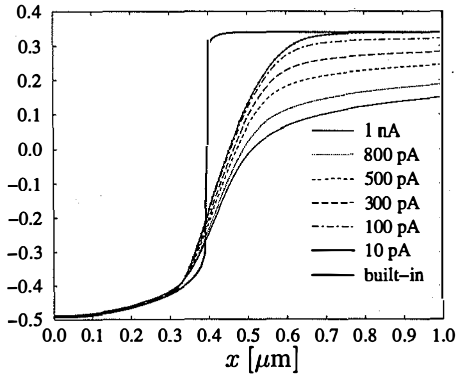

Figure 3. Surface potential of the p^+n test device.

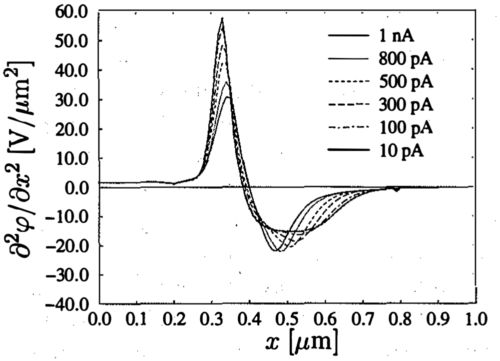

Figure 4. Second derivative of the surface potential for the p^+n device.

beam currents some sort of inverse modeling is necessary for proper delineation of the pn-junction. Simulation of AVC measurements has proven a capable tool for developing methods for pn-junction extraction.

[1] W. Werner, H. Lakatha, H. Smith, L. LeTarte, V. Ambrose, and J. Baker, "Auger Voltage Contrast Imaging for the Delineation of 2-Dimensional Junctions in Cross-sectioned MOS Devices," *J.Vac.Sci.Technol.*, accepted for publication 1998.

[2] T. Simlinger, H. Kosina, M. Rottinger, and S. Selberherr, "MINIMOS-NT: A Generic Simulator for Complex Semiconductor Devices," in *25th European Solid State Device Research Conference* (H. de Graaff and H. van Kranenburg, eds.), pp. 83–86, 1995.

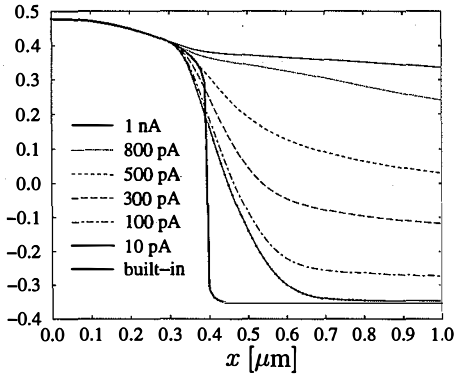

Figure 5. Surface potential of the n^+p test device.

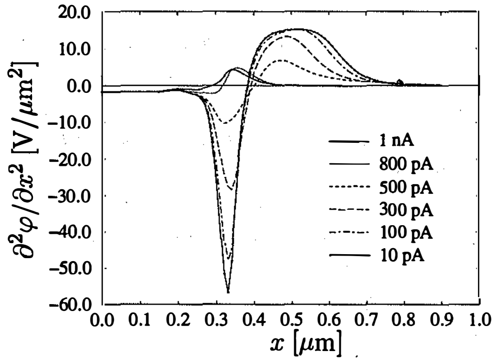

Figure 6. Second derivative of the surface potential for the n^+p device.

[3] D. Kyser and D. Wittry, "Spatial Distribution of Excess Carriers in Electron-Beam Excited Semiconductors," *Proc.IEEE*, pp. 733–734, May 1967.

[4] H. Wagner, A. Pfeiffer, C. Schiebl, and W. Werner, "Monte Carlo Simulation of Electron Scattering for Arbitrary 2D Structures Using a Modified Quadtree Geometry Discretization.," *Microchim. Acta*, vol. 13, p. 533, 1995.